Published in final edited form as:
Circ Res. 2013 March 1; 112(5): 849–862. doi:10.1161/CIRCRESAHA.111.300158.

Rotors and the Dynamics of Cardiac Fibrillation

Sandeep V. Pandit and **José Jalife**
Center for Arrhythmia Research Dept. of Internal Medicine-Cardiology University of Michigan, Ann Arbor

Abstract

The objective of this article is to present a broad review on the role of cardiac electrical rotors and their accompanying spiral waves in the mechanism of cardiac fibrillation. At the outset, we present a brief historical overview regarding reentry, and then discuss the basic concepts and terminologies pertaining to rotors and their initiation. Thereafter, the intrinsic properties of rotors and spiral waves, including phase singularities, wavefront curvature and dominant frequency maps are discussed. The implications of rotor dynamics for the spatio-temporal organization of fibrillation, independent of the species being studied are touched upon next. The knowledge gained regarding the role of cardiac structure in the initiation and/or maintenance of rotors and the ionic bases of spiral waves in the last two decades, and its significance for drug therapy is reviewed subsequently. We conclude by looking at recent evidence suggesting that rotors are critical in sustaining both atrial and ventricular fibrillation (AF, VF) in the human heart, and its implications for treatment with radio-frequency ablation.

Keywords

atrial fibrillation; ventricular fibrillation; Spiral waves; wavefront curvature; wavebreak

Introduction

The term “rotor” is becoming a household name in cardiac electrophysiology. It applies to the organizing source of functional reentrant activity, particularly in the context of tachycardia and fibrillation. Emerging evidence clearly supports a major role for rotors as the drivers of cardiac fibrillation in both animal models and in humans. Remarkably, much of what we have learned about the dynamics of rotors and of the spiral waves generated by them derives from the field of computational biology, and from the study of wave propagation in excitable media. In the heart, the atria and ventricles share similar dynamics of electrical wave propagation despite their vastly different geometry, global structure and ionic mechanisms. More important, the behaviors of the electrical rotors and spiral waves that form in their respective walls are also similar and may be analyzed using tools derived from the study of non-linear systems. Thus, in the following lines, we make an attempt to reconcile such concepts with the more traditional ideas about mechanisms of cardiac

Correspondence: Dr. José Jalife Center for Arrhythmia Research University of Michigan NCRC, 2800, Plymouth Road Ann Arbor, MI 48109 jjalife@med.umich.edu.

Disclosures: S. Pandit: Research Grant from Gilead, Inc J. Jalife: Research Grant from Gilead, Inc.; Scientific Advisory board for Topera, Inc; Scientific Advisory Board for Rhythm Solutions, Inc.

fibrillation. But first we set our current knowledge of reentry in a historical context, and then briefly define the basic notions and the terminology that is used throughout the article. Subsequently, we review our current understanding of how rotors are initiated, and the technologies that are used to localize them in the atria or ventricles, as well as to quantify their properties, including their dynamics and frequency of activation. We then present evidence demonstrating the high similarities in the dynamics of rotors and their consequences that exists in all mammals, including man. Here we pay attention to universal scaling laws that may govern such similarities. Thereafter, we focus on triggers and substrate as the essential factors involved, respectively, in the mechanisms of initiation and maintenance of rotors, followed by the ionic bases of rotor dynamics and the manner in which antiarrhythmic drugs can modify rotor behavior. We close the article by briefly looking into new evidence supporting the idea that rotors may be critical in sustaining both atrial and ventricular fibrillation (AF, VF) in the human heart, and the manner in which such evidence might lead to more mechanistic approaches to effectively terminate AF in the clinical electrophysiology laboratory.

Evolving theories about reentry over the last century

This topic has been reviewed in detail recently.[1] Only the main points are highlighted here. Studies on fibrillation and its mechanisms have been carried out since the turn of the 20th century. The first known experiments were conducted by Mayer in jellyfish rings and turtle ventricular muscle in 1906.[2] In Mayer's experiments, isolated rings of muscle could sustain circulating activity for long periods of time. Shortly thereafter, the studies of Mines and Garrey in rings of canine ventricular muscle formed the basis for the concept of anatomical reentry as we know it today.[3-5] Lewis postulated that AF and atrial flutter could be attributed to a circulating reentrant wavefront which encroached upon its own partially refractory tail.[6-8] The main difference between fibrillation and flutter was the gap or the nature of the encroachment of the front into the tail: the gap was fully excitable and quite large in flutter, whereas it was smaller and partially excitable in AF, because of intermingled front and tail. These ideas progressed forward in the 1940s with the theoretical studies of Wiener and Rosenblueth, who postulated that reentry around an obstacle was necessary to sustain fibrillation.[9] In the 1960s, Moe challenged the prevalent concepts about reentry, by postulating that instead of a single reentrant circuit, multiple, randomly propagating wavelets were responsible for sustaining AF.[10] Remarkably, Moe's hypothesis was partly based on results obtained via innovative computer modeling studies.[11] In the 1970s, Allessie proposed the "leading circle" hypothesis based on experiments conducted in the rabbit atrial muscle, in which electrical waves rotated around a functional obstacle.[12-14] Subsequently, in 1985, Allessie and colleagues provided the first experimental proof for Moe's multiple wavelet hypothesis of AF in the canine atria.[15] The concept of rotors generating spiral waves was meanwhile being developed in parallel via theoretical studies conducted in the erstwhile USSR by Krinsky and others, and in the US by Winfree.[16,17] It was proposed that these reverberators or rotors could also exist in the heart, and underlie functional reentry. The first experimental demonstration of a spiral wave in the heart was made in an isolated sheep ventricular muscle slice by Davidenko and colleagues in 1990.[18] This was mainly possible thanks to the use of voltage sensitive dyes, which allowed for high-resolution mapping of the cardiac electrical activity.[19] The subsequent two decades have seen a vast amount of knowledge gained regarding rotors, spiral waves and their underlying mechanisms, partly due to the development of sophisticated tools and algorithms for their analyses, which has led to our current concepts regarding rotors and their role in cardiac fibrillation.[1,20,21] There is still debate about the precise mechanisms of fibrillation (small number of driving sources or rotors, versus multiple wavelets).[1,21-24] Nevertheless, the concept of rotors as underlying drivers of fibrillation has driven the field forward, and is poised to prove immensely beneficial as both basic science and clinical investigators use

these ideas in developing mechanism-based therapies and treatment modalities for AF and VF in the next decade.

What is a rotor?

The traditional view of a wave propagating in a fixed ring-like path, with an excitable gap separating the wave front from its tail of refractoriness (Fig. 1A) [25] is an accurate representation of anatomical reentry. In this model, the wavelength is defined as the spatial extension of the propagating wave (all the depolarized cells), and computed as the product of the refractory period (RP) and the conduction velocity (CV). Functional reentry, on the other hand, was initially described via the leading circle hypothesis (Fig. 1B).[14] According to this model, there is no fully excitable gap as the circulating excitation wavefront encroaches upon its tail. The tissue inside the leading circle is deemed to receive centripetal excitation wavefronts, which render it refractory. A rotor is a similar form of functional reentrant activity (Fig. 1C), but with a critical difference: the curved wavefront and wavetail meet each other, at a singularity (white asterisk, Fig. 1C), and the tissue at the center is not refractory.[26] The terms spiral wave and rotor have been used interchangeably by some; however in the context of cardiac arrhythmias, rotors are “drivers” or organizing sources of fibrillation, be it AF or VF, and a spiral wave is more accurately a 2D representation of the curved vortices generated by the spinning rotor in its immediate surroundings.[1] The 3D representation of a spiral wave is termed a “scroll wave”, and its center of rotation is a hollow filament formed by the revolving trajectory of the spiral tip (Fig. 1D). The latter represents the core of the spiral viewed from one surface, as depicted with the broken circle in Fig.1E. The presence of both scroll waves and filaments has been demonstrated in the heart in both numerical[27] and experimental studies.[28]

A schematic representation of a rotor generating spiral waves is illustrated in Fig. 1E, to allow for a closer look at the curved activation wavefront, the curved wavetail and the point at which wavefront and wavetail meet. The wavefront represents an area of depolarized cells as the cardiac impulse travels forward, and the wavetail is made up of the group of cells that have undergone full excitation (action potential upstroke), and are returning to rest (action potential repolarization). As discussed in detail below, in 1998, Gray et al developed a technique based on phase plane analysis to investigate cardiac fibrillation in optical mapping experiments, and identify the rotor, which was demonstrated to be a singularity point or phase singularity (PS), represented in Fig. 1E by an asterisk.[29] This allowed for the tracking of the spiral and its tip dynamics, in space, over time. When a rotor is stationary, it pivots as a PS around a circular trajectory forming the “core” of the spiral wave (Fig. 1E); however, when the rotor meanders, its trajectory can take various complex shapes, depending upon the tissue excitability.[30] As noted above, the 3D representation of a spiral wave is the scroll wave. If the rotor is completely stationary and spans from the epicardium to the endocardium, the filament of the spiral would be a linear cylinder (I-shaped).[28] The filament can also bend, adopting varying non-linear shapes (L-shaped; U-shaped; O-shaped; etc).[27] If, on the other hand, the scroll wave meanders, the phase singularity would not form a cylinder, but move along a trajectory whose complexity will depend on the degree of meandering. In this case, the filament would be a line.

Three important points of difference become immediately apparent between the theory of rotors and the so-called leading circle reentry: First, the leading circle idea does not consider the curvature of the rotating wavefront[31] as a factor controlling the velocity of the impulse and the dynamics of the reentrant activity. The theory of rotors envisions that the propagation velocity of a wavefront in the 2- or 3-dimensional myocardium very much depends on its curvature; waves whose front is concave propagate faster than planar waves but the velocity of planar waves is faster than convex waves. Rotating waves consist of

wavefronts, and the curvature progressively increases toward the center (the core). At the very tip (the PS) the convex curvature reaches a critical value that makes it impossible for the activity to invade the core. This leads to the second difference; the leading circle assumes full refractoriness at the core, produced by the continuing invasion of centripetal waves forming a ring of excitation around a functionally unexcitable obstacle, not unlike the anatomical obstacle of circus movement reentry a la Mines.[4] Whether functional or anatomical, the obstacle at the center of the leading circle would make it impossible for the reentry circuit to meander or drift. In contrast, rotors can meander because they pivot around unexcited but eminently excitable tissue.[32] As such, the mechanism underlying the rotation does not depend upon the refractoriness at the core, but on the exceedingly steep wavefront curvature at the PS, which slows conduction to a critical level that renders the wavefront unable to invade the core.[20] Third, unlike the leading circle, there is no "fixed" wavelength in rotor generated spiral waves. In fact, the expanse between the wavefront and the wavetail varies, increasing as a function of the distance (as one goes away) from the PS (Fig. 1E). This is because electrotonic gradients established between cells at the core and cells in the near vicinity shorten significantly the action potentials of cells near the core.[25] The above point is particularly important, since concepts regarding wavelength prolongation are frequently used in the literature, such as for quantifying the effects of antiarrhythmic drugs.[33-35] The spiral wave properties remind us that the wavelength is variable, and should be used with caution. More accurate quantification of drug effects on reentry would be obtained by studying how the drug changes the spinning frequency of the rotor (discussed later), as well as its degree of meandering and the number of wavebreaks its spiraling waves undergo in the periphery, as it happens in fibrillatory conduction.[36]

Another important concept in reentry is the so-called "excitable gap".[37] Analyzing the rotor and spiral wave properties allows one to discern this variable in a clear, quantifiable fashion, as shown in Fig. 1F. This figure shows a snapshot of a simulated rotor generated in a 2D sheet, that incorporated numerical ionic models of human atrial cells.[38] Each cell in the sheet mimics the electrical action potential phenotype seen in persistent AF.[39,40] The top panel shows a snapshot of membrane voltage distribution in the sheet. One can appreciate how current from a depolarized group of cells (red/orange, representing the wavefront) invades the resting cells/tissue in front of it (in dark blue). The bottom panel shows a plot of the product of the variables "h.j", which represent the fast (h) and slow inactivation variables (j) of the Na^+ current, I_{Na},[41] which is the main ionic current driving the spiral wavefront. These variables represent the availability of I_{Na}, and their value varies between 0.0 and 1.0. In other words, when "h.j" is 0.0, no I_{Na} is available, and the tissue in unexcitable (the white area in the bottom panel of Fig. 1F), whereas a value of 1.0 means that the tissue is fully available for excitation. All other values between 1.0 and 0.0 represent the "excitable tissue or gap", where I_{Na} is available, and a stimulus in this area may elicit a response. Thus the excitable gap underlying a spiral in a 2D sheet is also seen to take a spiral shape (Fig. 1F).

Initiation of rotors and spiral waves via vortex shedding

A rotor may be initiated in multiple ways.[30] This can involve standard cross-field stimulation protocols in theoretical studies,[38,42] where a plane wave, generated by a linear stimulus applied at one side of a cardiac tissue sheet, is followed by a second stimulus applied perpendicularly while the tissue is only partially recovered. The 2nd stimulus, when timed appropriately, and when located spatially in the refractory tail of the 1st wavefront, can lead to wavebreak and initiate a rotor. Similarly, a rotor can be initiated by unidirectional conduction block in cardiac tissue resulting from tissue heterogeneities in excitability, repolarization or conduction velocity,[43] or even dynamical properties such as action potential alternans.[44] The underlying basis for rotor and spiral wave initiation is also

explained by the phenomenon known as “vortex shedding”,[46] which occurs when a wave encounters an obstacle with sharp edges. Vortex shedding is analogous to the formation of eddies and turbulence, when a water flow reaches a bifurcation or interacts with a narrow barrier, and is rooted in the concept of critical curvature.[45] In brief, as discussed above, a planar wavefront propagates faster than a convex wavefront; in fact the greater the wavefront curvature the slower the conduction velocity, up to a critical level at which propagation cannot occur (see below).

The mechanism of vortex shedding was explained by Cabo et al on the basis of the concept of wavefront curvature (R).[46] Fig 2A shows a schematic representation of R, at a time when the wavefront (white) reaches the edge of the obstacle (red). The white curve bounds the area adjacent to the obstacle, which needs to propagate to the left in order to circumnavigate the obstacle. The radius R of this area is comparable to the width of the wavefront, which determines whether that wavefront (i.e., the source) will be able to excite the tissue ahead of it (i.e., the sink). In a series of experiments and concomitant simulations, Cabo and colleagues demonstrated the principle of wavebreak generated by vortex shedding.[46] In simulations, they utilized a 2D sheet of ventricular cells incorporating the Luo-Rudy-1991 kinetics.[47] For experiments, they used a thin slice of sheep ventricular epicardium; the slice was perfused with a voltage sensitive dye and optically mapped.[46] An artificial linear obstacle was etched into the ventricular muscle sheet in both simulations and experiments (depicted in a cartoon in Fig. 2B, where the obstacle is represented by a red line). As illustrated by the top panel of Fig. 2C (condition I), when the excitability of the tissue was normal and a wave was initiated by a point stimulus near the lower right margin of the obstacle (asterix), the wavefront proceeded to circumnavigate the obstacle without breaking or detaching from it, eventually extinguishing after activating the entire sheet.[46] As shown by the lower panel of Fig. 2C, when the excitability of the tissue was diminished somewhat (condition II), either by reducing the maximum conductance of I_{Na} by 75% in simulations, or by superfusing the tissue with the sodium channel blocker tetrodotoxin in experiments, the same stimulation protocol yielded completely different results: now the wavefront moved upward but detached from the obstacle, curled and began to rotate around its broken tip, generating a vortex.[46] In the top panel of Fig. 2C (condition I) R is larger than the minimum radius of excitation, or critical curvature R_{Cr}. Under these conditions the front progresses laterally without detachment, successfully circumnavigating the obstacle. When $R < R_{Cr}$, (condition II) then the wavefront curls, eventually detaching from the obstacle to generate a vortex around a PS. From the study of Cabo et al.,[46] one can infer how pathophysiological conditions such as ischemia or an infarct in the ventricles, or atrial remodeling due to persistent AF, where both I_{Na} density and excitability are reduced and numerous obstacles in the form of patchy fibrotic tissue exist,[48-50] set the stage for initiation of the rotors that maintain tachycardia or fibrillation.

The inability of the excitation wavefront to depolarize tissue at the PS and its tendency to curve underlies rotor initiation, and is important in rotor maintenance as well.[46] The latter is demonstrated in Fig. 2D, in which the normalized conduction velocity of the spiral excitation wavefront is plotted versus the distance from its tip (red line, in the z-axis).[1] It can be seen that the wavefront curvature is highest at the tip, and this results in a lesser conduction velocity near the rotation center. Away from the tip, the curvature is reduced, and the normalized conduction velocity increases.[1] At the tip, there is constant sink-source mismatch in play, which causes the rotor to pivot or to meander in complex trajectories; if enough excitable tissue is available, sustained reentry will occur. Thus wavefront curvature related sink-to-source mismatch at the tip is responsible for both rotor initiation (vortex shedding) and maintenance.

Phase mapping of rotors and singularities

A step forward in the analysis of rotor dynamics was the development of the phase mapping technique by Gray and colleagues in 1998.[29] Fig. 3A shows a typical optical signal recorded from a point on the epicardial surface of a rabbit heart during VF. We call this time series F(t), where "t" is time. In Fig. 3B, the same signal was plotted in two-dimensional phase space, as $F(t+\tau)$ versus F(t), where τ is an embedded delay. This approach revealed trajectories rotating around a circle in the center. Then a phase variable "θ" was computed at each site on the cardiac surface, and was defined as $\theta(t) = \arctan(F(t+\tau) - F_{mean}, F(t) - F_{mean})$, where F_{mean} = threshold value, defined as mean value of 4 seconds of VF activity, and τ $1/4^{th}$ the value of the cycle length during fibrillation.

Phase mapping allowed for the generation of color phase movies and the quantification of rotor dynamics which led to the clear identification of phase singularity points, as illustrated in Fig. 3C. Each color represents a phase in the excitation recovery cycle and a phase singularity is defined as a site where all phases converge because at the PS the phase is arbitrary; in contrast, the surrounding elements exhibit a continuous progression of phase that is equal to $\pm 2\pi$ around the PS.[29] The original approach of plotting the dynamics on phase space has allowed investigators to systematically study the initiation, maintenance and termination of rotors, in normal and pathophysiological conditions.[51] However, the approach requires a careful choice of the embedded delay τ. More recently, a Hilbert Transform (HT)-based approach facilitated computing the instantaneous phase.[52,53] Regardless of the approach, it is clear that wavebreak and formation of a PS is an essential condition for a rotor to exist. Moreover we have learned through experiments and simulations that rotors need not be stationary but meander over complex trajectories,[54] giving rise to irregular electrograms (Figure 3D)[55]. In many cases fibrillation is terminated because of a PS colliding with a boundary,[42,51] thereby extinguishing the spiral waves.

Dominant frequency mapping

In the late 1990s/early 2000s, experimental mapping of both AF and VF in isolated hearts of various animal models using optical imaging demonstrated that rotors, whether single, or in small numbers, or sometimes multiple, were consistently detected during cardiac reentry.[56,57] It was possible to visualize not only the rotors, but phase mapping allowed one to track their spatiotemporal dynamics, revealing that rotors were either stable, as in monomorphic ventricular tachycardia, or constantly meandered over complex trajectories as in polymorphic ventricular tachycardia.[51] The latter were also postulated to underlie both torsade de pointes,[58] as well as VF.[59] A further important development in the analysis of rotors occurred when their time-dependent behavior was analyzed in the frequency domain.[60] Fast Fourier transform (FFT) analysis of optical signals within a given time window across vast extensions of the epicardial surface of the fibrillating atria or ventricles yielded a spatial frequency map of the signals in the area of interest.[57,60,61] Selecting the maximum frequency in the Fourier spectrum of each recording location allowed for the construction of so-called dominant-frequency (DF) maps, as shown in Fig. 4.[61] Examples, of optical and electrical signals from the left (LA) and the right (RA) sheep atria and their respective power spectra obtained during AF induced via burst pacing in the presence of acetylcholine are shown (Fig. 4A-D). The 3-second time-dependent signals are on the left, and their corresponding frequency spectra obtained after FFT analysis are on the right. Although multiple peaks of frequency can be observed in the individual spectra, dominant peaks of frequency can be identified in all. In Fig. 4E, DF peaks from multiple locations recorded with a CCD camera in a 5-sec optical mapping movie are plotted as DF maps superimposed on a schematic representation of the sheep LA and RA.[61] A consistent finding in power spectral analyses obtained in this manner was that in a vast majority of the

experiments the frequency of atrial activation during AF was higher in the LA compared to the RA, This finding has been replicated for AF in other species such as pigs,[62] and also in the electrogram analysis of AF frequencies for paroxysmal AF in humans.[63-65]

Thus representation of fibrillation in the frequency domain demonstrates that AF[61] (and also VF[66]) rather than being the result of randomly propagating wavelets, shows a consistent spatial organization of frequencies, which is chamber dependent. This has led to the following postulates, 1. A spatially distributed hierarchy of dominant frequencies of excitation indicates that, in most cases, AF is sustained by a small number of high frequency drivers (rotors) in the LA that maintain the overall activity. 2. The DF of the rotor(s) is exceedingly high and therefore can only drive in a 1:1 fashion the tissue in its immediate surroundings. Beyond this 1:1 domain, the wavefronts undergo intermittent, spatially distributed wavebreaks, the end result being fibrillatory conduction toward distal areas in both the LA and the RA.[1,61,67] Thus dominant frequency analysis of experimental data provided evidence for organization in some forms of fibrillation,[68] and this experimental observation was also supported by computer simulations,[69] as well as by mapping of rotors in 2D monolayers of rat neonatal ventricular cells, as shown in Fig 4F-I.[70] In this representative experiment the bottom half of the monolayer was infected with an adenoviral construct for the gene coding hERG, the molecular correlate of the rapid delayed rectifier K^+ current, I_{Kr}, whereas the top half was uninfected. This resulted in an I_{Kr} density gradient with higher I_{Kr} current magnitude in the bottom half and sustained rotor formation (Fig. 4F).[70] The spiral wavefronts generated by the rotor in the I_{Kr} infected region blocked intermittently at the interface and could not drive the uninfected region in a 1:1 fashion. Instead, as shown by the DF map in Fig. 4G, a frequency gradient was established, with a higher DF in the infected region compared to the uninfected region. These results are similar to the LA-RA gradients in cholinergic AF experiments in sheep (see Fig. 4E),[60,61] and paroxysmal AF in humans.[63-65] Further, when a “regularity index” (RI), defined as the ratio of DF to total spectral power was calculated for each video camera pixel recording the potentiometric dye fluorescence changes in the 2D monolayer, the values were unequally distributed. A vertical line (X-X’) drawn in the 2D monolayer dish (Fig. 4H) showed the RI to be lowest at the interface between the infected and the uninfected regions (Fig. 4I).[70] These data suggests that the most complex “fractionation” of the signal is observed at the interface/boundary between the hERG infected and non-infected regions, where there is a sharp change in refractoriness (due to changes in density of I_{Kr}). Altogether, dominant frequency mapping has allowed for the demonstration that fibrillation is deterministic and displays organization, with a hierarchy of frequencies indicating underlying chamber-specific ion channel gradients, and the location of complex fractionated signals, which are at the periphery of the rotors.

Universal scaling of fibrillation frequency

Mechanisms of fibrillation are being investigated in many laboratories using hearts from a variety of species, ranging from the mouse to much larger mammals, including dogs, sheep, goats, pigs, as well as explanted human hearts. Thus an important question arises as to whether rotors can be observed across different species, and whether the rotor properties obey common laws. The question is motivated in part by the long-held contention that fibrillation cannot sustain in tissue whose mass is lower than critical.[71] This idea was first challenged by the studies of Vaidya and colleagues, who showed that, with burst pacing, one could create conditions in small mouse hearts for functional reentry and sustained VF, and that rotors could be observed in an area as small as 100 mm^2.[72] By the mid-2000s, rotors and spiral waves had been demonstrated in isolated hearts from mice, rats, guinea pigs, rabbits, sheep, pigs and dogs. To understand their common link, Noujaim and colleagues endeavored to quantify the relationship between body mass and VF frequencies.[73] They

were partly motivated by earlier studies, where it was shown that many biological phenomena such as metabolic rate, life span, respiratory rate and ECG parameters like the PR interval scale with body mass.[74] The general relationship being $Y = a\times (\text{body mass})^b$, where Y is the biological variable of interest, "a" is a constant, and "b" represents the scaling exponent.[73] Results obtained by Noujaim et al are reproduced in Fig. 5. Panel A shows DF maps obtained in optical experiments during VF in a mouse, a guinea pig, a rabbit and a human whose body weights were 30 g, 600 g, 3 Kg and 90 Kg, respectively. In each map, the dominant frequency domain is indicated in red: 38 Hz for the mouse, 26 Hz for the guinea pig, 15 Hz for the rabbit and 6.8 Hz for the human heart. Notice that while the body weight changes 4 orders of magnitude from mouse to human, the DF changes only one order of magnitude. In Fig. 5B, a meta-analysis of data collected from 40 studies in 11 different species, from mouse to horse, are plotted as VF frequency versus body mass (BM) on a double logarithmic graph.[73] Fitting the data points revealed that VF frequency $\approx 18.9 \times BM^{-1/4}$; in other words, VF cycle length turned out to be $\approx 53.0 \times BM.^{1/4}$ Thus, analysis of VF in the frequency domain allowed for an all-inclusive pattern to emerge across mammalian species. The underlying mechanisms have not been elucidated completely, but it seems clear that changes in the species-related action potential duration along with the heart size play a significant role.[73]

Triggers, cardiac structure and the formation and maintenance of rotors

The onset and maintenance of cardiac fibrillation require an event (trigger) that initiates the arrhythmia and the presence of a predisposing substrate that perpetuates it. In AF, well-known clinical studies have demonstrated that the vast majority of ectopic discharges initiating the arrhythmia emerge from the pulmonary vein (PV) sleeves,[75] which are known to terminate in dead-end pathways. In some patients, the electrical properties of the muscle bundles in the PV sleeves seem to make them highly prone to generate high-frequency automatic or triggered discharges, which propagate into the posterior left atrial (LA) wall whose highly heterogeneous and anisotropic fiber bundle arrangements and abrupt changes in thickness[76] provide an ideal substrate for sink-to-source mismatch, wavebreak and reentry formation. In a recent study in which brief trains of electrical stimuli were used to trigger PV discharges at a high frequency, most of the wavebreaks that initiated AF appeared at the septal side of the septopulmonary bundle near the right superior pulmonary vein, where the myocardial thickness dramatically expands.[77] It was clear that the source current provided by certain PV impulses was insufficient to overcome the vast sink of the transition posterior LA-septum, which resulted in wavebreak, reentry, and AF. A somewhat different but related mechanism can initiate reentry and fibrillation in the ventricles. For example, at the Purkinje-muscle junction[78], anatomic expansions are prone to conduction delays and block specifically in areas of abrupt electric current source-to-sink mismatch.[79] As discussed above for the study of Cabo et al,[46] whether in the atria or ventricles, source-to-sink unbalance can explain wave detachment from obstacles and vortex shedding leading to rotors and fibrillation.

Once initiated, rotors will spin at very high rates to generate electrical turbulence (fibrillatory conduction). Recently, using a chronic RA tachypacing model of persistent AF in the sheep, along with continuous cardiac rhythm monitoring by dual implantable devices, we demonstrated that rotors are capable of maintaining cardiac fibrillation in the long term, even after both structural and electrical remodeling have taken place.[80] We demonstrated that in-vivo DF values during AF progressively increased while preserving in the long-term a DF difference between the left and the right atria. After follow-up periods of 9-24 weeks, mapping of the atria and subsequent structural analyses ex-vivo confirmed the presence of DF gradients from posterior LA to RA, together with patterns of activation, all of which was consistent with the contention that rotors in an enlarged left atrium are fully capable of

maintaining AF dynamics in the long term. Similar to AF, the papillary muscle ventricular structures have been postulated to play an important role in the generation and maintenance of both VF and VT.[81]

The importance of structure in initiating reentry and arrhythmias was further re-iterated in recent experiments in monolayers of neonatal rat ventricular myocyte (NRVM) cultures. Auerbach et al showed that in patterned monolayers consisting of two wide regions connected by a thin isthmus, reflection and arrhythmogenesis was enhanced.[82] The Tung lab showed that reentry is readily induced by rapid pacing in NRVM monolayers containing a central and asymmetric island containing a predefined zigzag pattern.[83]

Ionic bases of rotors

Many investigators using either pharmacological tools in experimental animal models or numerical simulations have contributed to our current understanding of the underlying ionic bases for the initiation and maintenance of rotors (only a few are cited here because of space limitations).[84-94] However, the availability of genetic mouse models,[95] and the reproducibility of consistent rotors in 2D monolayers of neonatal rat cells,[96,97] coupled with the development of biophysically-detailed ionic mathematical models of murine ventricular electrophysiology[98,99]allowed for a more robust dissection of the contribution of individual ion channels to high frequency rotors from the year 2000 onwards. In this section we discuss mainly studies carried out in our laboratory over the last decade, although we acknowledge the important contributions of numerous other investigators to this particular field. [87-94]

The earliest studies focused on the role of the inward rectifier K^+ channel, I_{K1}. Computer modeling studies of 2D reentry[100] and experimental studies in guinea pig hearts[66] suggested an important role for I_{K1} in the spatio-temporal organization of VF frequencies across different chambers of the heart. The importance of I_{K1} received further support from studies which showed that VF frequencies were slowed, and VF was subsequently terminated by $BaCl_2$ at concentrations of 1–50 μM, which were relatively selective for I_{K1} blockade.[84] The chamber-specific, LA-RA spatiotemporal gradient of AF frequencies in the presence of acetylcholine was attributable to different densities of another inward rectifier K^+ channel, the acetylcholine-activated K^+ current, I_{KACh}.[67] The density of I_{K1} was also found to be upregulated in atrial myocytes isolated from chronic AF patients.[101-103] When computer simulations were conducted to examine the consequences of I_{K1} increase, the rotors were found to be faster, and the tip meander was reduced, being confined to a smaller area, thus stabilizing fibrillation.[38] Those simulations suggested, that in addition to causing a shorter action potential duration (APD), I_{K1} accelerated rotors by increasing the availability of I_{Na}; this was possible due to the hyperpolarization of the resting membrane potential (V_{rest}) by I_{K1}. Although this hyperpolarization was small (~5 mV), the change in V_{rest} occurred over the steep portion of the availability curve for I_{Na}, and thus resulted in a dramatic acceleration of the rotor.

The first direct demonstration of the role of I_{K1} was made possible when transgenic (TG) mice in which I_{K1} was overexpressed became available.[104] Sustained rotors induced in isolated TG mouse hearts were very long-lasting (> 1 hour) and extremely fast (~50-60 Hz); by contrast, in wild-type (WT) hearts, rotors were much slower (~20-25 Hz) and lasted less than ~10 sec.[105] In Fig. 6A, we compare the activation map of a rotor observed experimentally in a TG mouse with I_{K1} overexpression (right) versus a WT heart (left). It is clear that the rotor completes one rotation much earlier in the TG mouse (note the different time scales). These experimental results were confirmed in computer simulations, using a detailed ionic mathematical model of the mouse ventricular action potential, which incorporated all the major K^+ currents recorded experimentally.[105] The simulations further

supported a key role for I_{K1}, and I_{Na} as important ionic mechanisms determining fast rotor activity.

Although relevant, the studies in mouse did not reveal the role of the 2 main repolarizing K^+ currents in the human ventricle, i.e. the fast and the slow delayed rectifier K^+ currents, viz. I_{Kr} and I_{Ks}.[106] These currents do not contribute in a meaningful way to the short APD in the mouse ventricle.[106] Studies in higher mammalian hearts did show that E-4031, a relatively selective blocker of I_{Kr}, could slow VF frequencies.[94] Further, in a rabbit model of 2D reentry created via cryoablation of the ventricular endocardium it was shown that perfusion of nifekalant, a relatively selective blocker of I_{Kr}, terminated rotors mostly due to their collision with the atrio-ventricular groove.[93] Therefore, we investigated the role of these delayed rectifier K^+ currents in monolayers of confluent, electrically coupled NRVM, using an approach modified from that described originally by the Kleber Lab.[96] At 5-6 days of age, the action potential of NRVMs present a plateau and APD of approximately 200 msec, which would allow both I_{Kr} and I_{Ks} to activate. To further increase the density of either I_{Ks} or I_{Kr}, we used adenoviral transfer of genomic sequences of either KvLQT1-minK, or hERG, respectively in NRVM monolayers, and studied their effects on rotor dynamics.[107,108] To our surprise, I_{Ks} overexpression did not increase rotor frequency at all, but over time, the excessive I_{Ks} caused an increasing number of wavebreaks to occur. This is illustrated in Fig 6B by the representative phase maps in a control monolayer, and a monolayer in which I_{Ks} was overexpressed.[107] Experiments in HEK cells and computer simulations suggested that the increased wavebreak incidence observed in monolayers was due to the phenomenon of post-repolarization refractoriness, due to residual outward I_{Ks} current, following the action potential.[107] This phenomenon was demonstrated in guinea pig ventricular myocytes in the late 1980s before.[109,110]

In Fig. 6C, overexpression of I_{Kr} caused the rotor to accelerate significantly, compared to control.[107] Concomitant simulations showed that the acceleration due to I_{Kr} increase was not comparable to that caused by I_{K1} overexpression.[108] Interestingly, both simulations and experiments showed a novel mechanism underlying rotor acceleration, in addition to APD shortening: transient V_{rest} hyperpolarization, which again would indirectly affect rotor frequency by modifying I_{Na} availability.[108] The Tung lab conducted similar experiments with overexpression of I_{K1} in rat neonatal monolayers,[111] which supported the conclusions from our mouse studies.[105]

In addition to K^+ channels, the Ca^{2+} channels and the E-C coupling machinery also influence the cardiac action potential and repolarization,[112] and both are also likely to influence the spiral wave dynamics, although the results remain controversial. In one study from our lab which examined the effect of verapamil on VF, the DF was reduced, core meander was increased, and VF was converted to ventricular tachycardia (VT).[85] However, these results must be interpreted with caution, since at the concentrations of verapamil used in this study, verapamil blocks both the L-type Ca^{2+} channel, I_{CaL}, as well as I_{Kr}.[113] The role of intracellular Ca^{2+} ($[Ca^{2+}]_i$) in sustaining VF/spirals is also less clear and remains controversial. Studies from the Zaitsev lab suggested that $[Ca^{2+}]_i$ -action potential dissociation during VF was a consequence, not a cause of wavebreaks in VF, and that no spontaneous voltage-independent $[Ca^{2+}]_i$ waves could be seen.[114,115] However, others have challenged these findings.[116] In contrast, $[Ca^{2+}]_i$ has been shown to be important in the initiation of spontaneous activity in TdP,[117] and inherited arrhythmias such as catecholaminergic polymorphic ventricular tachycardia (CPVT), which can then give rise to the initiation of rotors and fibrillation.[118] Finally, the Na^+ current, I_{Na} is key is determining excitability and the upstroke of the cardiac action potentials, and is the main current driving the wavefront during normal propagation, as well as during rotor activity. We have assessed the role of I_{Na} in rotor dynamics either directly via TTX, which blocks I_{Na},[86,119] or

indirectly by elevating concentrations of extracellular K^+ ($[K^+]_o$)[42,62] or simulating conditions of global ischemia,[119] which limit the availability of I_{Na} due to a depolarized resting membrane potential. In every case, a reduced I_{Na} decreased the DF of the rotor, and increased its meander. If I_{Na} was blocked sufficiently (by TTX or ($[K^+]_o$), the rotor was terminated by collision with a boundary, abolishing AF or VF. However, in many instances, antiarrhythmic class I drugs that block I_{Na}, such as quinidine do not always terminate fibrillation, but either sustain it,[58] or convert it to VT (unpublished observations). Indeed, TG mice with ablation of *SCN5A*, the gene coding $Na_V1.5$ which is the molecular correlate of I_{Na}, display increased susceptibility to arrhythmogenesis, including VT/VF.[120]

Antiarrhythmic drugs and rotors

A direct consequence of the increase in the knowledge of the ionic mechanisms of rotors has been to understand how this information can be applied to design/select more efficacious antiarrhythmic drugs to treat cardiac fibrillation. As discussed above, I_{K1} and I_{Na} seem to have dominant effects on reentry properties (frequency, meander). Thus we have begun to investigate drugs that can block these channels, particularly I_{K1}, and examine their putative effects on reentrant activity. In one study, we compared the effects of chloroquine, an antimalarial drug, to that of quinidine, a class I antiarrhythmic, on VF and rotor dynamics.[121] Fig. 7A shows DF maps during VF in a TG mouse heart overexpressing I_{K1}; the top panel shows the effect of quinidine, whereas the bottom panel depicts the effect of chloroquine; the former reduced VF frequency, but did not terminate the arrhythmia, whereas the latter restored sinus rhythm.[121] The normalized DF in the absence and presence of quinidine/chloroquine are shown in an aggregate of experiments, and demonstrate that chloroquine terminated VF in all experiments (Fig. 7B). Based on patch-clamp and molecular structure data, we hypothesize that the greater success for terminating VF in the case of chloroquine was in part due to its greater ability to block I_{K1}. Similar results were observed in a recent study conducted in a sheep model of stretch-induced AF.[122] Fig. 7C shows DF maps of the posterior left atrium during stretch-induced AF in an isolated heart before and after coronary perfusion of chloroquine; the drug reduced the rotor frequency.[122] These data were compared with those of flecainide, another class I antiarrhythmic, as summarized in Fig. 7D. Flecainide failed to terminate AF in any experiment, while converting AF to atrial tachycardia in 2/5 experiments at clinically relevant concentrations.[122] In contrast, chloroquine terminated AF and restored sinus rhythm in 7/7 experiments.[122] These initial experiments testify to the applicability of concepts learned through the theory of rotors as a mechanism of both AF and VF; i.e. drugs that block I_{K1} will likely have greater potency in abolishing cardiac fibrillation. These studies represent only a beginning, and would be strengthened by design of new drugs that can putatively block I_{Na}/I_{K1}, without being proarrhythmic, and are tested in different arrhythmia/pathophysiological models. An interesting corollary is the antiarrhythmic effect of regional cooling on the myocardium, which seems to reduce the frequency and then terminate VF by unpinning of rotors, which then drift toward the periphery, away from the cooled region, and extinguish by subsequent collision with a boundary.[123]

Spirals in the human heart

Most studies on rotors and their analysis until today have been confined to experimental animal models and numerical simulations. Computer modeling studies conducted in either simplified 2D sheets, or complex and geometrically realistic 3D models of the human atria and ventricles have demonstrated that it is possible to induce sustained rotors that drive both AF,[38,124] and VF.[125,126] However, experimental data from humans has been elusive and difficult to obtain. Recent *in vivo* and/or epicardial surface mapping studies in humans have demonstrated the presence of rotors during VF.[53,126] Nanthakumar and colleagues have

demonstrated the presence of rotors,[73,127] or even scroll waves[128] during early VF with electrical/optical mapping in Langendorff-perfused human hearts. An optically mapped rotor on the human ventricular epicardial surface is shown[73] (Fig. 8A). Another case in point is the recent work of Narayan et al, who have used basket catheters to demonstrate sustained sources, a majority of them consisting of rotors, as key driving mechanisms underlying persistent AF. [129] This study showed that patients with persistent AF had a higher number of sources, and also had a shorter cycle length, compared to with patients in paroxsymal AF.[129] An example of a rotor in the left atrium generating fibrillatory conduction in the right atrium during AF is shown in Fig. 8B.[129] Even more remarkably, the authors could target these spirals via catheter-based radiofrequency ablation, and slow down or terminate AF in a manner of minutes rather than hours, as is typically the case.[130] These initial reports are intriguing and exciting: they provide the first support for the role of rotors as key drivers of sustained AF in humans. If reproduced consistently by other laboratories, this mechanistically based approach could substantially improve the safety and the outcome of radiofrequency ablation and benefit many patients.

Summary

Emerging evidence clearly supports a major role for rotors as the drivers of cardiac fibrillation in animal models and in humans. It is our prediction that in the next decade, more reliable and high resolution methods/devices will be developed to identify rotors and spiral waves consistently during AF and VF *in vivo*. These studies will immensely benefit ablation and electrical/defibrillator therapies in the short term. But we expect that as more mechanistic insights on the ionic/molecular bases of rotors continue to emerge, novel, more efficacious and safer therapeutic approaches (either preventive or curative) will eventually come of age to provide relief from the debilitating and potentially lethal effects of rotors/ fibrillation in less expensive ways to a much larger population worldwide.

Acknowledgments

We would like to thank Kate Campbell and Sergey Mironov for assistance with some of the figures.

Funding Sources: Supported by NHLBI Grants P01HL039707, P01HL087226, Gilead Inc., and the Leducq Foundation (to Dr. José Jalife), and by Gilead Inc. (to Dr. Sandeep V. Pandit).

Non-standard Abbreviations and Acronyms

AF	atrial fibrillation
APD	Action potential duration
BM	body mass CV. conduction velocity
DF	dominant frequency
FFT	fast Fourier transform
HT	Hilbert transform
h	fast inactivation variable of the sodium current
j	slow inactivation variable of the sodium current
LA	left atrium
NRVM	neonatal rat ventricular myocyte
PS	phase singularity

PV	pulmonary vein
RA	right atrium
R	radius of wavefront curvature
R_{Cr}	critical radius of wavefront curvature
RP	refractory period
TG	transgenic
VF	ventricular fibrillation
VT	ventricular tachycardia
V_{rest}	resting membrane potential

References

1. Jalife J. Déjà vu in the theories of atrial fibrillation dynamics. Cardiovasc Res. Mar 1; 2011 89(4): 766–75. Epub 2010 Nov 19. Review. [PubMed: 21097807]
2. Mayer, A. Rhythmical Pulsation in Scyphomedusae. Carnegie Institute of Washington; Washington, DC: 1906. p. 1-62.Publication number 47
3. Mines GR. On dynamic equilibrium in the heart. J Physiol. 1913; 46:349–383. [PubMed: 16993210]
4. Mines G. On circulating excitations in heart muscles and their possible relation to tachycardia and fibrillation. Trans R Soc Can. 1914; 4:43–52.
5. Garrey W. The nature of fibrillary contraction of the heart: its relation to tissue mass and form. Am J Physiol. 1914; 33:397–414.
6. Lewis T. Oliver-Sharpey lectures on the nature of flutter and fibrillation of the auricle. Lecture II. Auricular Fibrillation. Br Med J. 1921; 1:590–593.
7. Lewis T. Oliver-Sharpey lectures on the nature of flutter and fibrillation of the auricle. Lecture I. Auricular Flutter. Br Med J. 1921; 1:551–555. [PubMed: 20770255]
8. Lewis T. Observations upon flutter and fibrillation. II. The nature of auricular flutter. Heart. 1920; 7:191–233.
9. Wiener N, Rosenblueth A. The mathematical formulation of the problem of conduction of impulses in a network of connected excitable elements, specifically in cardiac muscle. Arch Inst Cardiol Mex. 1946; 16:205–265. [PubMed: 20245817]
10. Moe G. On the multiple wavelet hypothesis of atrial fibrillation. Arch Int Pharmacodyn Ther. 1962; 140:183–188.
11. Moe GK, Rheinboldt WC, Abildskov JA. A computer model of atrial fibrillation. Am Heart J. 1964; 67:200–220. [PubMed: 14118488]
12. Allessie MA, Bonke FI, Schopman FJ. Circus movement in rabbit atrial muscle as a mechanism of trachycardia. Circ Res. Jul; 1973 33(1):54–62. [PubMed: 4765700]
13. Allessie MA, Bonke FI, Schopman FJ. Circus movement in rabbit atrial muscle as a mechanism of tachycardia. II. The role of nonuniform recovery of excitability in the occurrence of unidirectional block, as studied with multiple microelectrodes. Circ Res. Aug; 1976 39(2):168–77. [PubMed: 939001]
14. Allessie MA, Bonke FI, Schopman FJ. Circus movement in rabbit atrial muscle as a mechanism of tachycardia. III. The “leading circle” concept: a new model of circus movement in cardiac tissue without the involvement of an anatomical obstacle. Circ Res. Jul; 1977 41(1):9–18. [PubMed: 862147]
15. Allessie, MA.; Lammers, WJEP.; Bonke, FIM.; Hollen, J. Experimental evaluation of Moe’s multiple wavelet hypothesis of atrial fibrillation. In: Zipes, DP.; Jalife, J., editors. Cardiac Electrophysiology and Arrhythmias. Grune & Stratton; Orlando: 1985. p. 265-275.
16. Krinsky V. Spread of excitation in an inhomogeneous medium (state similar to cardiac fibrillation). Biophysics. 1966; 11:676–683.

17. Winfree, AT. When Time Breaks Down. Princeton University Press; Princeton: 1987.
18. Davidenko JM, Kent PF, Chialvo DR, Michaels DC, Jalife J. Sustained vortex-like waves in normal isolated ventricular muscle. Proc Natl Acad Sci USA. 1990; 87:8785–8789. [PubMed: 2247448]
19. Salama G, Morad M. Merocyanine 540 as an optical probe of transmembrane electrical activity in the heart. Science. 1976; 191:485–487. [PubMed: 1082169]
20. Jalife J. Ventricular fibrillation: mechanisms of initiation and maintenance. Annu Rev Physiol. 2000; 62:25–50. Review. [PubMed: 10845083]
21. Jalife J, Berenfeld O, Skanes A, Mandapati R. Mechanisms of atrial fibrillation: mother rotors or multiple daughter wavelets, or both? J Cardiovasc Electrophysiol. Aug; 1998 9(8 Suppl):S2–12. Review. [PubMed: 9727669]
22. Witkowski FX, Leon LJ, Penkoske PA, Giles WR, Spano ML, Ditto WL, Winfree AT. Spatiotemporal evolution of ventricular fibrillation. Nature. Mar 5; 1998 392(6671):78–82. [PubMed: 9510250]
23. Eckstein J, Verheule S, de Groot NM, Allessie M, Schotten U. Mechanisms of perpetuation of atrial fibrillation in chronically dilated atria. Prog Biophys Mol Biol. Jun-Jul;2008 97(2-3):435–51. [PubMed: 18378284]
24. Tabereaux PB, Dosdall DJ, Ideker RE. Mechanisms of VF maintenance: wandering wavelets, mother rotors, or foci. Heart Rhythm. Mar; 2009 6(3):405–15. [PubMed: 19251220]
25. Jalife J. Inward rectifier potassium channels control rotor frequency in ventricular fibrillation. Heart Rhythm. Nov; 2009 6(11 Suppl):S44–8. Epub 2009 Sep 1. Review. [PubMed: 19880073]
26. Vaquero M, Calvo D, Jalife J. Cardiac fibrillation: from ion channels to rotors in the human heart. Heart Rhythm. Jun; 2008 5(6):872–9. Epub 2008 Apr 9. Review. [PubMed: 18468960]
27. Berenfeld O, Pertsov AM. Dynamics of intramural scroll waves in three-dimensional continuous myocardium with rotational anisotropy. J Theor Biol. Aug 21; 1999 199(4):383–94. [PubMed: 10441456]
28. Yamazaki M, Mironov S, Taravant C, Brec J, Vaquero LM, Bandaru K, Avula UM, Honjo H, Kodama I, Berenfeld O, Kalifa J. Heterogeneous atrial wall thickness and stretch promote scroll waves anchoring during atrial fibrillation. Cardiovasc Res. Apr 1; 2012 94(1):48–57. [PubMed: 22227155]
29. Gray RA, Pertsov AM, Jalife J. Spatial and temporal organization during cardiac fibrillation. Nature. Mar 5; 1998 392(6671):75–8. [PubMed: 9510249]
30. Panfilov AV. Zipes DP, Jalife J. Theory of Reentry. Chapter 31. Cardiac Electrophysiology: From Cell to Bedside (5th edition). 2009
31. Fast VG, Kléber AG. Role of wavefront curvature in propagation of cardiac impulse. Cardiovasc Res. Feb; 1997 33(2):258–71. Review. [PubMed: 9074688]
32. Gray RA, Jalife J, Panfilov AV, Baxter WT, Cabo C, Davidenko JM, Pertsov AM. Mechanisms of cardiac fibrillation. Science. Nov 17; 1995 270(5239):1222–3. [PubMed: 7502055]
33. Blaauw Y, Gögelein H, Tieleman RG, van Hunnik A, Schotten U, Allessie MA. “Early” class III drugs for the treatment of atrial fibrillation: efficacy and atrial selectivity of AVE0118 in remodeled atria of the goat. Circulation. Sep 28; 2004 110(13):1717–24. [PubMed: 15364815]
34. Wijffels MC, Dorland R, Allessie MA. Pharmacologic cardioversion of chronic atrial fibrillation in the goat by class IA, IC, and III drugs: a comparison between hydroquinidine, cibenzoline, flecainide, and d-sotalol. J Cardiovasc Electrophysiol. Feb; 1999 10(2):178–93. [PubMed: 10090222]
35. Wang J, Bourne GW, Wang Z, Villemaire C, Talajic M, Nattel S. Comparative mechanisms of antiarrhythmic drug action in experimental atrial fibrillation. Importance of use-dependent effects on refractoriness. Circulation. Sep; 1993 88(3):1030–44. [PubMed: 8353865]
36. Jalife J, Berenfeld O, Mansour M. Mother rotors and fibrillatory conduction: a mechanism of atrial fibrillation. Cardiovasc Res. May; 2002 54(2):204–16. Review. [PubMed: 12062327]
37. Wijffels MC, Dorland R, Mast F, Allessie MA. Widening of the excitable gap during pharmacological cardioversion of atrial fibrillation in the goat: effects of cibenzoline, hydroquinidine, flecainide, and d-sotalol. Circulation. Jul 11; 2000 102(2):260–7. [PubMed: 10889140]

38. Pandit SV*, Berenfeld O*, Anumonwo JMB, Zaritski RM, Kneller J, Nattel S, Jalife J. Ionic Determinants of Functional Reentry in a 2-D Model of Human Atrial Cells During Simulated Chronic Atrial Fibrillation. Biophys. J. 2005; 88:3806–3821. [PubMed: 15792974]
39. Courtemanche M, Ramirez RJ, Nattel S. Ionic mechanisms underlying human atrial action potential properties: insights from a mathematical model. Am J Physiol. Jul; 1998 275(1 Pt 2):H301–21. [PubMed: 9688927]
40. Courtemanche M, Ramirez RJ, Nattel S. Ionic targets for drug therapy and atrial fibrillation-induced electrical remodeling: insights from a mathematical model. Cardiovasc Res. May; 1999 42(2):477–89. [PubMed: 10533583]
41. Luo CH, Rudy Y. A dynamic model of the cardiac ventricular action potential. I. Simulations of ionic currents and concentration changes. Circ Res. Jun; 1994 74(6):1071–96. [PubMed: 7514509]
42. Pandit SV*, Warren M*, Mironov S, Tolkacheva EG, Kalifa J, Berenfeld O, Jalife J. Mechanisms Underlying the Antifibrillatory Action of Hyperkalemia in Guinea Pig Hearts. Biophys. J. May 19; 2010 98(10):2091–2101. [PubMed: 20483316]
43. Weiss JN, Qu Z, Chen PS, Lin SF, Karagueuzian HS, Hayashi H, Garfinkel A, Karma A. The dynamics of cardiac fibrillation. Circulation. Aug 23; 2005 112(8):1232–40. [PubMed: 16116073]
44. Fox JJ, Riccio ML, Hua F, Bodenschatz E, Gilmour RF Jr. Spatiotemporal transition to conduction block in canine ventricle. Circ Res. Feb 22; 2002 90(3):289–96. [PubMed: 11861417]
45. Cabo C, Pertsov AM, Davidenko JM, Jalife J. Electrical turbulence as a result of the critical curvature for propagation in cardiac tissue. Chaos. Mar; 1998 8(1):116–126. [PubMed: 12779715]
46. Cabo C, Pertsov AM, Davidenko JM, Baxter WT, Gray RA, Jalife J. Vortex shedding as a precursor of turbulent electrical activity in cardiac muscle. Biophys J. Mar; 1996 70(3):1105–11. [PubMed: 8785270]
47. Luo CH, Rudy Y. A model of the ventricular cardiac action potential. Depolarization, repolarization, and their interaction. Circ Res. Jun; 1991 68(6):1501–26. [PubMed: 1709839]
48. Janse MJ, Wit AL. Electrophysiological mechanisms of ventricular arrhythmias resulting from myocardial ischemia and infarction. Physiol Rev. Oct; 1989 69(4):1049–169. [PubMed: 2678165]
49. Nattel S, Burstein B, Dobrev D. Atrial remodeling and atrial fibrillation: mechanisms and implications. Circ Arrhythm Electrophysiol. Apr; 2008 1(1):62–73. Review. [PubMed: 19808395]
50. Schotten U, Verheule S, Kirchhof P, Goette A. Pathophysiological mechanisms of atrial fibrillation: a translational appraisal. Physiol Rev. Jan; 2011 91(1):265–325. [PubMed: 21248168]
51. Gray RA. Zipes DP, Jalife J. Rotors and Spiral waves in the heart. Chapter 33. Cardiac Electrophysiology: From Cell to Bedside (5th edition). 2009
52. Bray MA, Wikswo JP. Considerations in phase plane analysis for nonstationary reentrant cardiac behavior. Phys Rev E Stat Nonlin Soft Matter Phys. May.2002 65(5 Pt 1):051902. [PubMed: 12059588]
53. Nash MP, Mourad A, Clayton RH, Sutton PM, Bradley CP, Hayward M, Paterson DJ, Taggart P. Evidence for multiple mechanisms in human ventricular fibrillation. Circulation. 2006; 114:536–542. [PubMed: 16880326]
54. Davidenko JM, Pertsov AV, Salomonsz R, Baxter W, Jalife J. Stationary and drifting spiral waves of excitation in isolated cardiac muscle. Nature. Jan; 1992 23;355(6358):349–51.
55. Zlochiver S, Yamazaki M, Kalifa J, Berenfeld O. Rotor meandering contributes to irregularity in electrograms during atrial fibrillation. Heart Rhythm. Jun; 2008 5(6):846–54. [PubMed: 18534369]
56. Skanes AC, Mandapati R, Berenfeld O, Davidenko JM, Jalife J. Spatiotemporal periodicity during atrial fibrillation in the isolated sheep heart. Circulation. Sep 22; 1998 98(12):1236–48. [PubMed: 9743516]
57. Chen J, Mandapati R, Berenfeld O, Skanes AC, Jalife J. High-frequency periodic sources underlie ventricular fibrillation in the isolated rabbit heart. Circ Res. Jan 7-21; 2000 86(1):86–93. [PubMed: 10625309]
58. Asano Y, Davidenko JM, Baxter WT, Gray RA, Jalife J. Optical mapping of drug-induced polymorphic arrhythmias and torsade de pointes in the isolated rabbit heart. J Am Coll Cardiol. Mar; 1997 15;29(4):831–42. PubMed PMID: 9091531.

59. Jalife J, Gray R. Drifting vortices of electrical waves underlie ventricular fibrillation in the rabbit heart. Acta Physiol Scand. Jun; 1996 157(2):123–31. [PubMed: 8800352]
60. Berenfeld O, Mandapati R, Dixit S, Skanes AC, Chen J, Mansour M, Jalife J. Spatially distributed dominant excitation frequencies reveal hidden organization in atrial fibrillation in the Langendorff-perfused sheep heart. J Cardiovasc Electrophysiol. Aug; 2000 11(8):869–79. [PubMed: 10969749]
61. Mansour M, Mandapati R, Berenfeld O, Chen J, Samie FH, Jalife J. Left-to-right gradient of atrial frequencies during acute atrial fibrillation in the isolated sheep heart. Circulation. May 29; 2001 103(21):2631–6. [PubMed: 11382735]
62. Pandit SV*, Zlochiver S*, Filgueiras-Rama D, Mironov S, Yamazaki M, Ennis SR, Noujaim S, Workman AJ, Berenfeld O, Kalifa J, Jalife J. Targeting Atrio-Ventricular Differences in Ion Channel Properties for Terminating Acute Atrial Fibrillation in Pigs. Cardiovasc. Res. 2011; 89(4):843–51. [PubMed: 21076156]
63. Lazar S, Dixit S, Marchlinski FE, Callans DJ, Gerstenfeld EP. Presence of left-to-right atrial frequency gradient in paroxysmal but not persistent atrial fibrillation in humans. Circulation. Nov; 2004 16;110(20):3181–6.
64. Sanders P, Berenfeld O, Hocini M, Jais P, Vaidyanathan R, Hsu LF, Garrigue S, Takahashi Y, Rotter M, Sacher F, Scavee C, Ploutz-Snyder R, Jalife J, Haissaguerre M. Spectral analysis identifies sites of high-frequency activity maintaining atrial fibrillation in humans. Circulation. Aug; 2005 9;112(6):789–97.
65. Atienza F, Almendral J, Jalife J, Zlochiver S, Ploutz-Snyder R, Torrecilla EG, Arenal A, Kalifa J, Fernandez-Aviles F, Berenfeld O. Real-time dominant frequency mapping and ablation of dominant frequency sites in atrial fibrillation with left-to-right frequency gradients predicts long-term maintenance of sinus rhythm. Heart Rhythm. Jan; 2009 6(1):33–40. [PubMed: 19121797]
66. Samie FH, Berenfeld O, Anumonwo J, Mironov SF, Udassi S, Beaumont J, Taffet S, Pertsov AM, Jalife J. Rectification of the background potassium current: a determinant of rotor dynamics in ventricular fibrillation. Circ Res. Dec; 2001 7;89(12):1216–23.
67. Sarmast F, Kolli A, Zaitsev A, Parisian K, Dhamoon AS, Guha PK, Warren M, Anumonwo JM, Taffet SM, Berenfeld O, Jalife J. Cholinergic atrial fibrillation: I(K,ACh) gradients determine unequal left/right atrial frequencies and rotor dynamics. Cardiovasc Res. Oct 1; 2003 59(4):863–73. [PubMed: 14553826]
68. Jalife J. Rotors and spiral waves in atrial fibrillation. J Cardiovasc Electrophysiol. Jul; 2003 14(7): 776–80. Review. [PubMed: 12930260]
69. Kalifa J, Tanaka K, Zaitsev AV, Warren M, Vaidyanathan R, Auerbach D, Pandit S, Vikstrom KL, Ploutz-Snyder R, Talkachou A, Atienza F, Guiraudon G, Jalife J, Berenfeld O. Mechanisms of wave fractionation at boundaries of high-frequency excitation in the posterior left atrium of the isolated sheep heart during atrial fibrillation. Circulation. Feb; 2006 7;113(5):626–33.
70. Campbell KF, Calvo CJ, Mironov S, Herron T, Berenfeld O, Jalife J. Spatial gradients in action potential duration created by regional magnetofection of hERG are a substrate for wavebreak and turbulent propagation in a rat cardiomyocyte monolayer model of cardiac fibrillation. J Physiol. Oct 22.2012 [Epub ahead ofprint].
71. Zipes DP, Fischer J, King RM, Nicoll A deB, Jolly WW. Termination of ventricular fibrillation in dogs by depolarizing a critical amount of myocardium. Am J Cardiol. Jul; 1975 36(1):37–44. [PubMed: 1146696]
72. Vaidya D, Morley GE, Samie FH, Jalife J. Reentry and fibrillation in the mouse heart. A challenge to the critical mass hypothesis. Circ Res. Jul; 1999 23;85(2):174–81.
73. Noujaim SF, Berenfeld O, Kalifa J, Cerrone M, Nanthakumar K, Atienza F, Moreno J, Mironov S, Jalife J. Universal scaling law of electrical turbulence in the mammalian heart. Proc Natl Acad Sci U S A. Dec; 2007 26;104(52):20985–9.
74. Noujaim SF, Lucca E, Muñoz V, Persaud D, Berenfeld O, Meijler FL, Jalife J. From mouse to whale: a universal scaling relation for the PR Interval of the electrocardiogram of mammals. Circulation. Nov; 2004 2;110(18):2802–8.

75. Haïssaguerre M, Jaïs P, Shah DC, Takahashi A, Hocini M, Quiniou G, Garrigue S, LeMouroux A, LeMétayer P, Clémenty J. Spontaneous initiation of atrial fibrillation by ectopic beats originating in the pulmonary veins. N Engl J Med. Sep 3; 1998 339(10):659–66. [PubMed: 9725923]
76. Ho SY, Cabrera JA, Sanchez-Quintana D. Left atrial anatomy revisited. Circ Arrhythm Electrophysiol. Feb; 2012 5(1):220–8. [PubMed: 22334429]
77. Klos M, Calvo D, Yamazaki M, Zlochiver S, Mironov S, Cabrera JA, Sanchez-Quintana D, Jalife J, Berenfeld O, Kalifa J. Atrial septopulmonary bundle of the posterior left atrium provides a substrate for atrial fibrillation initiation in a model of vagally mediated pulmonary vein tachycardia of the structurally normal heart. Circ Arrhythm Electrophysiol. Aug; 2008 1(3):175–83. [PubMed: 19609369]
78. Moe GK, Mendez C. Functional block in the intraventricular conduction system. Circulation. Jun; 1971 43(6):949–54. [PubMed: 5578868]
79. Fast VG, Kléber AG. Cardiac tissue geometry as a determinant of unidirectional conduction block: assessment of microscopic excitation spread by optical mapping in patterned cell cultures and in a computer model. Cardiovasc Res. May; 1995 29(5):697–707. [PubMed: 7606760]
80. Filgueiras-Rama D, Price NF, Martins RP, Yamazaki M, Avula UM, Kaur K, Kalifa J, Ennis SR, Hwang E, Devabhaktuni V, Jalife J, Berenfeld O. Long-Term Frequency Gradients during Persistent Atrial Fibrillation in Sheep are Associated with Stable Sources in the Left Atrium. Circ Arrhythm Electrophysiol. Oct 10.2012 [Epub ahead of print].
81. Kim YH, Xie F, Yashima M, Wu TJ, Valderrábano M, Lee MH, Ohara T, Voroshilovsky O, Doshi RN, Fishbein MC, Qu Z, Garfinkel A, Weiss JN, Karagueuzian HS, Chen PS. Role of papillary muscle in the generation and maintenance of reentry during ventricular tachycardia and fibrillation in isolated swine right ventricle. Circulation. Sep; 1999 28;100(13):1450–9.
82. Auerbach DS, Grzda KR, Furspan PB, Sato PY, Mironov S, Jalife J. Structural heterogeneity promotes triggered activity, reflection and arrhythmogenesis in cardiomyocyte monolayers. J Physiol. May; 2011 1;589(Pt 9):2363–81.
83. Bian W, Tung L. Structure-related initiation of reentry by rapid pacing in monolayers of cardiac cells. Circ Res. Mar 3; 2006 98(4):e29–38. [PubMed: 16469953]
84. Warren M, Guha PK, Berenfeld O, Zaitsev A, Anumonwo JM, Dhamoon AS, Bagwe S, Taffet SM, Jalife J. Blockade of the inward rectifying potassium current terminates ventricular fibrillation in the guinea pig heart. J Cardiovasc Electrophysiol. Jun; 2003 14(6):621–31. [PubMed: 12875424]
85. Samie FH, Mandapati R, Gray RA, Watanabe Y, Zuur C, Beaumont J, Jalife J. A mechanism of transition from ventricular fibrillation to tachycardia : effect of calcium channel blockade on the dynamics of rotating waves. Circ Res. Mar 31; 2000 86(6):684–91. [PubMed: 10747005]
86. Kneller J, Kalifa J, Zou R, Zaitsev AV, Warren M, Berenfeld O, Vigmond EJ, Leon LJ, Nattel S, Jalife J. Mechanisms of atrial fibrillation termination by pure sodium channel blockade in an ionically-realistic mathematical model. Circ Res. Mar 18; 2005 96(5):e35–47. [PubMed: 15731458]
87. Comtois P, Sakabe M, Vigmond EJ, Munoz M, Texier A, Shiroshita-Takeshita A, Nattel S. Mechanisms of atrial fibrillation termination by rapidly unbinding Na+ channel blockers: insights from mathematical models and experimental correlates. Am J Physiol Heart Circ Physiol. Oct; 2008 295(4):H1489–504. [PubMed: 18676686]
88. Qu Z, Weiss JN. Effects of Na(+) and K(+) channel blockade on vulnerability to and termination of fibrillation in simulated normal cardiac tissue. Am J Physiol Heart Circ Physiol. Oct; 2005 289(4):H1692–701. [PubMed: 15937096]
89. Starmer CF, Romashko DN, Reddy RS, Zilberter YI, Starobin J, Grant AO, Krinsky VI. Proarrhythmic response to potassium channel blockade. Numerical studies of polymorphic tachyarrhythmias. Circulation. Aug 1; 1995 92(3):595–605. [PubMed: 7634474]
90. Blaauw Y, Schotten U, van Hunnik A, Neuberger HR, Allessie MA. Cardioversion of persistent atrial fibrillation by a combination of atrial specific and non-specific class III drugs in the goat. Cardiovasc Res. Jul 1; 2007 75(1):89–98. Epub 2007 Mar 30. [PubMed: 17466958] Cardiovasc Res. Nov 1.2007 76(2):373. Erratum in:

91. Wijffels MC, Dorland R, Allessie MA. Pharmacologic cardioversion of chronic atrial fibrillation in the goat by class IA, IC, and III drugs: a comparison between hydroquinidine, cibenzoline, flecainide, and d-sotalol. J Cardiovasc Electrophysiol. Feb; 1999 10(2):178–93. [PubMed: 10090222]

92. Ishiguro YS, Honjo H, Opthof T, Okuno Y, Nakagawa H, Yamazaki M, Harada M, Takanari H, Suzuki T, Morishima M, Sakuma I, Kamiya K, Kodama I. Early termination of spiral wave reentry by combined blockade of Na+ and L-type Ca2+ currents in a perfused two-dimensional epicardial layer of rabbit ventricular myocardium. Heart Rhythm. May; 2009 6(5):684–92. [PubMed: 19303369]

93. Yamazaki M, Honjo H, Nakagawa H, Ishiguro YS, Okuno Y, Amino M, Sakuma I, Kamiya K, Kodama I. Mechanisms of destabilization and early termination of spiral wave reentry in the ventricle by a class III antiarrhythmic agent, nifekalant. Am J Physiol Heart Circ Physiol. Jan; 2007 292(1):H539–48. [PubMed: 16936005]

94. Choi BR, Liu T, Salama G. The distribution of refractory periods influences the dynamics of ventricular fibrillation. Circ Res. Mar 16; 2001 88(5):E49–58. [PubMed: 11249880]

95. Nerbonne JM, Nichols CG, Schwarz TL, Escande D. Genetic manipulation of cardiac K(+) channel function in mice: what have we learned, and where do we go from here? Circ Res. Nov 23; 2001 89(11):944–56. Review. [PubMed: 11717150]

96. Rohr S, Schölly DM, Kléber AG. Patterned growth of neonatal rat heart cells in culture. Morphological and electrophysiological characterization. Circ Res. Jan; 1991 68(1):114–30. [PubMed: 1984856]

97. Bursac N, Aguel F, Tung L. Multiarm spirals in a two-dimensional cardiac substrate. Proc Natl Acad Sci U S A. Oct 26; 2004 101(43):15530–4. [PubMed: 15492227]

98. Pandit SV, Clark RB, Giles WR, Demir SS. A Mathematical Model of Action Potential Heterogeneity in Adult Rat Left Ventricular Myocytes. Biophys. J. 2001; 81(6):3029–51. [PubMed: 11720973]

99. Bondarenko VE, Szigeti GP, Bett GC, Kim SJ, Rasmusson RL. Computer model of action potential of mouse ventricular myocytes. Am J Physiol Heart Circ Physiol. Sep; 2004 287(3):H1378–403. [PubMed: 15142845]

100. Beaumont J, Davidenko N, Davidenko JM, Jalife J. Spiral waves in two-dimensional models of ventricular muscle: formation of a stationary core. Biophys J. Jul; 1998 75(1):1–14. [PubMed: 9649363]

101. Van Wagoner DR, Pond AL, McCarthy PM, Trimmer JS, Nerbonne JM. Outward K^+ current densities and Kv1.5 expression are reduced in chronic human atrial fibrillation. Circ Res. Jun; 1997 80(6):772–81. [PubMed: 9168779]

102. Dobrev D, Wettwer E, Himmel HM, Kortner A, Kuhlisch E, Schüler S, Siffert W, Ravens U. G-Protein beta(3)-subunit 825T allele is associated with enhanced human atrial inward rectifier potassium currents. Circulation. Aug 8; 2000 102(6):692–7. [PubMed: 10931811]

103. Voigt N, Trausch A, Knaut M, Matschke K, Varró A, Van Wagoner DR, Nattel S, Ravens U, Dobrev D. Left-to-right atrial inward rectifier potassium current gradients in patients with paroxysmal versus chronic atrial fibrillation. Circ Arrhythm Electrophysiol. Oct; 2010 1;3(5): 472–80.

104. Li J, McLerie M, Lopatin AN. Transgenic upregulation of IK1 in the mouse heart leads to multiple abnormalities of cardiac excitability. Am J Physiol Heart Circ Physiol. Dec; 2004 287(6):H2790–802. [PubMed: 15271672]

105. Noujaim SF, Pandit SV, Berenfeld O, Vikstrom K, Cerrone M, Mironov S, Zugermayr M, Lopatin AN, Jalife J. Up-regulation of the inward rectifier K+ current (I_{K1}) in the mouse heart accelerates and stabilizes rotors. J Physiol. Jan 1; 2007 578(Pt 1):315–26. [PubMed: 17095564]

106. Nerbonne JM, Kass RS. Molecular physiology of cardiac repolarization. Physiol Rev. Oct; 2005 85(4):1205–53. Review. [PubMed: 16183911]

107. Munoz V, Gzerda KR, Pandit SV, Mironov S, Taffet SM, Rohr S, Kleber AG, Jalife J. Adenoviral Expression of I_{Ks} contributes to wavebreak and fibrillatory conduction in neonatal rat ventricular cardiomyocyte monolayers. Circ. Res. Aug; 2007 101(5):475–83. [PubMed: 17626898]

108. Hou L, Deo M, Furspan P, Pandit SV, Auerbach D, Gong Q, Zhou Z, Berenfeld O, Jalife J. A Major Role for hERG in Determining Frequency of Reentry. Circ. Res. Dec 10; 2010 107(12): 1503–11. [PubMed: 20947828]

109. Delmar M, Glass L, Michaels DC, Jalife J. Ionic basis and analytical solution of the wenckebach phenomenon in guinea pig ventricular myocytes. Circ Res. Sep; 1989 65(3):775–88. PubMed PMID: 2766491. [PubMed: 2766491]

110. Delmar M, Michaels DC, Jalife J. Slow recovery of excitability and the Wenckebach phenomenon in the single guinea pig ventricular myocyte. Circ Res. Sep; 1989 65(3):761–74. [PubMed: 2475274]

111. Sekar RB, Kizana E, Cho HC, Molitoris JM, Hesketh GG, Eaton BP, Marbán E, Tung L. IK1 heterogeneity affects genesis and stability of spiral waves in cardiac myocyte monolayers. Circ Res. Feb 13; 2009 104(3):355–64. [PubMed: 19122180]

112. Bers, DM. Excitation-Contraction Coupling and Cardiac Contractile Force. Kluwer Academic Publishers; Dordrecht, The Netherlands: 2001.

113. Zhang S, Zhou Z, Gong Q, Makielski JC, January CT. Mechanism of block and identification of the verapamil binding domain to HERG potassium channels. Circ Res. May 14; 1999 84(9):989–98. [PubMed: 10325236]

114. Warren M, Zaitsev AV. Evidence against the role of intracellular calcium dynamics in ventricular fibrillation. Circ Res. May 9.2008 102(9):e103. PubMed. [PubMed: 18467634]

115. Warren M, Huizar JF, Shvedko AG, Zaitsev AV. Spatiotemporal relationship between intracellular Ca2+ dynamics and wave fragmentation during ventricular fibrillation in isolated blood-perfused pig hearts. Circ Res. Oct 26; 2007 101(9):e90–101. [PubMed: 17932324]

116. Ogawa M, Lin SF, Weiss JN, Chen PS. Calcium dynamics and ventricular fibrillation. Circ Res. Mar 14.2008 102(5):e52. [PubMed: 18340012]

117. Choi BR, Burton F, Salama G. Cytosolic Ca2+ triggers early afterdepolarizations and Torsade de Pointes in rabbit hearts with type 2 long QT syndrome. J Physiol. Sep 1; 2002 543(Pt 2):615–31. [PubMed: 12205194]

118. Cerrone M, Noujaim S, Talkachova A, Talkachou A, Berenfeld O, Anumonwo J, Pandit SV, Vikstrom K, Napolitano C, Priori SG, Jalife J. Arrhythmogenic mechanisms in a mouse model of catecholaminergic polymorphic ventricular tachycardia. Circ Res. Nov.2007 101(10):1039–48. [PubMed: 17872467]

119. Mandapati R, Asano Y, Baxter WT, Gray R, Davidenko J, Jalife J. Quantification of effects of global ischemia on dynamics of ventricular fibrillation in isolated rabbit heart. Circulation. Oct 20; 1998 98(16):1688–96. [PubMed: 9778336]

120. Papadatos GA, Wallerstein PM, Head CE, Ratcliff R, Brady PA, Benndorf K, Saumarez RC, Trezise AE, Huang CL, Vandenberg JI, Colledge WH, Grace AA. Slowed conduction and ventricular tachycardia after targeted disruption of the cardiac sodium channel gene Scn5a. Proc Natl Acad Sci U S A. Apr 30; 2002 99(9):6210–5. [PubMed: 11972032]

121. Noujaim SF, Stuckey JA, Ponce-Balbuena D, Ferrer-Villada T, López-Izquierdo A, Pandit SV, Sánchez-Chapula JA, Jalife J. Structural bases for the different anti-fibrillatory effects of chloroquine and quinidine. Cardiovasc Res. Mar 1; 2011 89(4):862–9. [PubMed: 21233253]

122. Filgueiras-Rama D, Martins RP, Mironov S, Yamazaki M, Calvo CJ, Ennis SR, Bandaru K, Noujaim SF, Kalifa J, Berenfeld O, Jalife J. Chloroquine terminates stretch-induced atrial fibrillation more effectively than flecainide in the sheep heart. Circ Arrhythm Electrophysiol. Jun 1; 2012 5(3):561–70. [PubMed: 22467674]

123. Yamazaki M, Honjo H, Ashihara T, Harada M, Sakuma I, Nakazawa K, Trayanova N, Horie M, Kalifa J, Jalife J, Kamiya K, Kodama I. Regional cooling facilitates termination of spiral-wave reentry through unpinning of rotors in rabbit hearts. Heart Rhythm. Jan; 2012 9(1):107–14. [PubMed: 21839044]

124. Krogh-Madsen T, Abbott GW, Christini DJ. Effects of electrical and structural remodeling on atrial fibrillation maintenance: a simulation study. PLoS Comput Biol. 2012; 8(2):e1002390. [PubMed: 22383869]

125. Bernus O, VanEyck B, Verschelde H, Panfilov AV. Transition from ventricular fibrillation to ventricular tachycardia: a simulation study on the role of Ca(2+)-channel blockers in human ventricular tissue. Phys Med Biol. Dec 7; 2002 47(23):4167–79. [PubMed: 12502041]

126. ten Tusscher KH, Mourad A, Nash MP, Clayton RH, Bradley CP, Paterson DJ, Hren R, Hayward M, Panfilov AV, Taggart P. Organization of ventricular fibrillation in the human heart: experiments and models. Exp Physiol. May; 2009 94(5):553–62. [PubMed: 19168541]

127. Massé S, Downar E, Chauhan V, Sevaptsidis E, Nanthakumar K. Ventricular fibrillation in myopathic human hearts: mechanistic insights from in vivo global endocardial and epicardial mapping. Am J Physiol Heart Circ Physiol. Jun; 2007 292(6):H2589–97. [PubMed: 17259437]

128. Nair K, Umapathy K, Farid T, Masse S, Mueller E, Sivanandan RV, Poku K, Rao V, Nair V, Butany J, Ideker RE, Nanthakumar K. Intramural activation during early human ventricular fibrillation. Circ Arrhythm Electrophysiol. Oct; 2011 4(5):692–703. [PubMed: 21750274]

129. Narayan SM, Krummen DE, Rappel WJ. Clinical mapping approach to diagnose electrical rotors and focal impulse sources for human atrial fibrillation. J Cardiovasc Electrophysiol. May; 2012 23(5):447–54. [PubMed: 22537106]

130. Narayan SM, Krummen DE, Shivkumar K, Clopton P, Rappel WJ, Miller JM. Treatment of Atrial Fibrillation by the Ablation of Localized Sources: CONFIRM (Conventional Ablation for Atrial Fibrillation With or Without Focal Impulse and Rotor Modulation) Trial. J Am Coll Cardiol. Jul 13.2012 [Epub ahead of print].

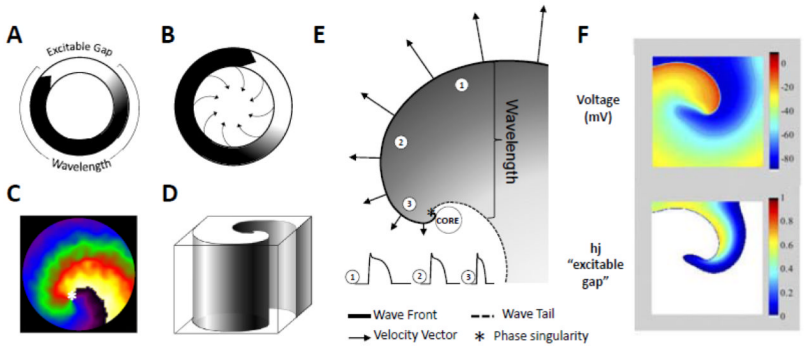

Figure 1.

Rotors and Spirals, Basic concepts. (A.) Schematic representation of reentry around a ring-like anatomical obstacle where the wavelength (black) is shorter than the path length allowing for a fully excitable gap (white). (B.) Leading circle reentry around a functional obstacle, with centripretal forces pointing inwards toward a refractory center. (C.) Two-dimensional spiral wave, along with the rotor tip at the center "*". (D.) Schematic of a three-dimensional scroll wave. (E.) Snapshot of the spiral wave: Electrotonic effects of the core decrease conduction velocity (arrows), action potential duration (representative examples shown from positions 1, 2 and 3) and wavelength (the distance from the wave front (black line) to the wave tail (dashed line)). Conduction velocity (CV) decreases and wavefront curvature becomes more pronounced, near the rotor, which is a phase singularity at the point where the wave front and the wave tail meet "*". (F.) Computer simulation of reentry (From Reference 38:). Top panel: snapshot of the transmembrane voltage distribution during simulated reentry in chronic AF conditions in a 2D sheet incorporating human atrial ionic math models. Bottom panel: snapshot of inactivation variables of sodium current, "h.j" during reentry.

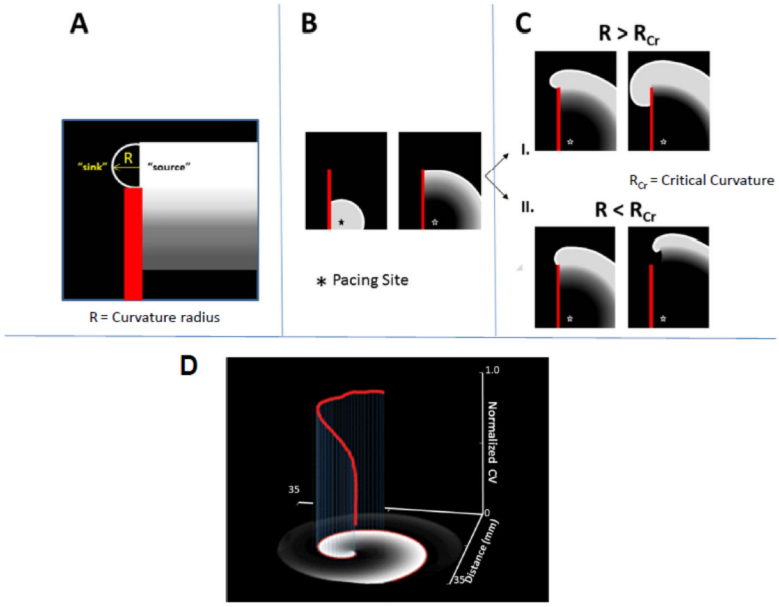

Figure 2.

Rotor initiation, vortex shedding. (A.) Schematic of the mechanism of detachment. Definition of the radius of curvature R, of the propagating wavefront (source) as it is about to invade the excitable, but non-excited tissue (sink) (B.) As a wave progresses along an obstacle (red line) the curvature of the wave at the edge of the obstacle will determine if the wave detaches. (C.) If the curvature of the wavefront (R) at the edge of the obstacle is greater than the critical curvature for detachment (RCr) the wave remains attached; if R is less than RCr the wave will detach from the obstacle and initiate reentry. (D.) Three-dimensional plot illustrating the effect the wavefront curvature at progressively shorter distances (x-,y-axis) from the core has on normalized conduction velocity (red, z-axis) in a Luo-Rudy computer simulation of reentry.

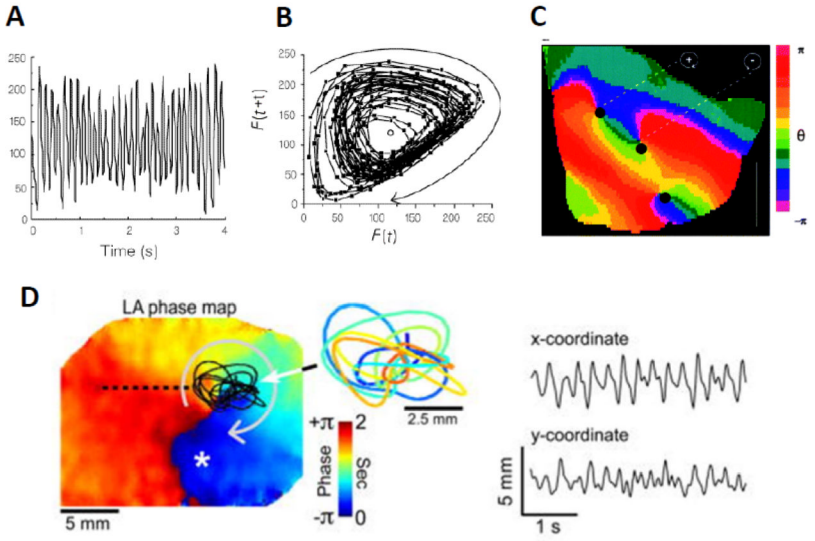

Figure 3.

From Reference 29) Singularity points revealed by phase plane analysis. (A.) Optical signal in time domain at a given point on the surface of a rabbit ventricle during VF.[29] (B.) Phase plane analysis, where optical signal with embedded delay F(t+τ) is plotted against itself F(t).[29] (C.) Phase movie during VF, with identification of rotors or phase singularities(PS), as dark black dots, at points where all phases (colors) converge. (D.) Rotor meandering and fractionation in optical mapping experiment during AF in isolated sheep heart. On the left, a left atrial phase snapshot demonstrates reentrant activity in the LA free wall. The inset shows the time-space trajectory of the tip; the x and y-coordinate signals are shown on the right. Modified from Zlochiver et al .[55]

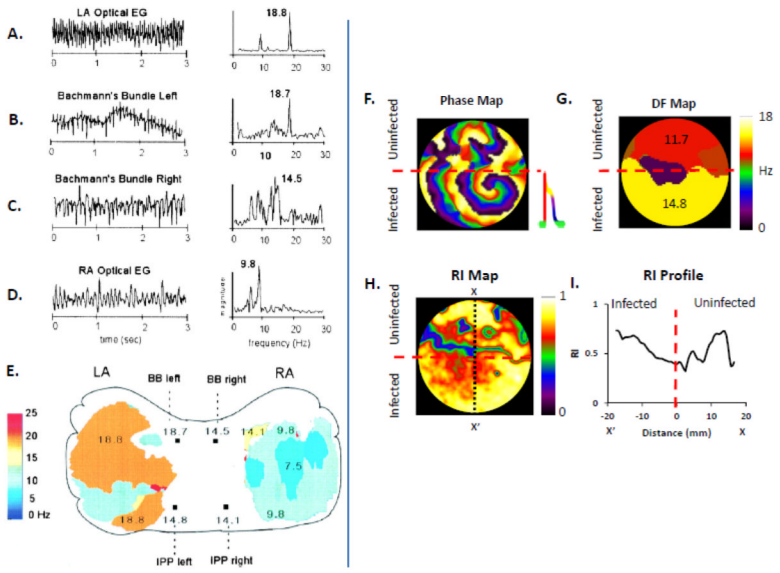

Figure 4.

Dominant frequency analysis of rotors and fibrillatory conduction. (A.-D.) Time-dependent optical signals and electrograms (left) and corresponding fast Fourier transform (FFT) right) from the left atrium (LA), Bachmann's Bundle (left), Bachmann's Bundle (right), and right atrium (RA) during AF induced in the presence of acetylcholine in an isolated, Langendorff-perfused sheep heart. (E.) Dominant Frequency (DF) map of areas within the LA and RA showing a Left-to-Right DF gradient during AF. (A-E: From reference 59) (F.) Phase map of a regionally ad-hERG infected neonatal rat ventricular myocyte monolayer showing a fast stable rotor within the infected region (below red dashed line) and patterns of wavebreak and fibrillatory conduction in the uninfected region (above red dashed line;)[70]. (G.) DF map demonstrating a frequency gradient between uninfected and hERG overexpressing regions, with an increased frequency of activation within the infected region. (H.) Regularity Index (RI) map showing a decrease (blue) in the regularity of activation at the hERG and APD gradient region. (I.) RI profile (taken at the black dotted line, along X-X') further illustrating that the region of greatest wave disruption occurs at the hERG/APD gradient (red dashed line).

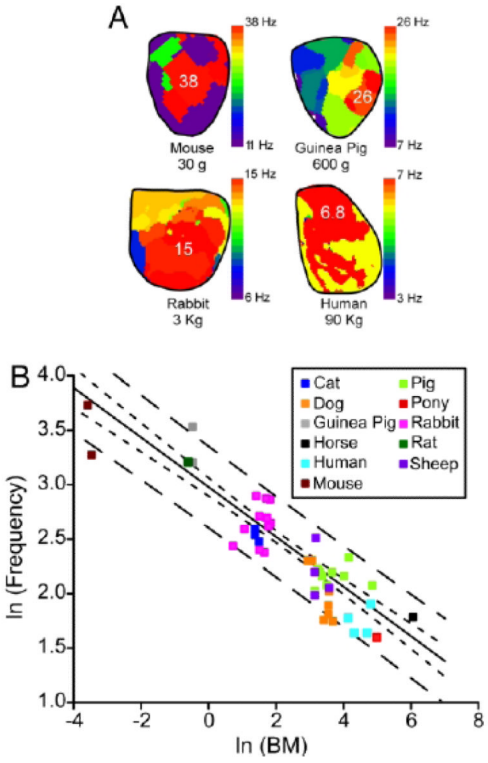

Figure 5.
Scaling of frequency of rotors anf fibrillation (From Reference 73). (A.) DF maps during VF in mouse, guinea pig, rabbit and humans. (B.) Double-logarithmic plot of DF versus body mass in different species.

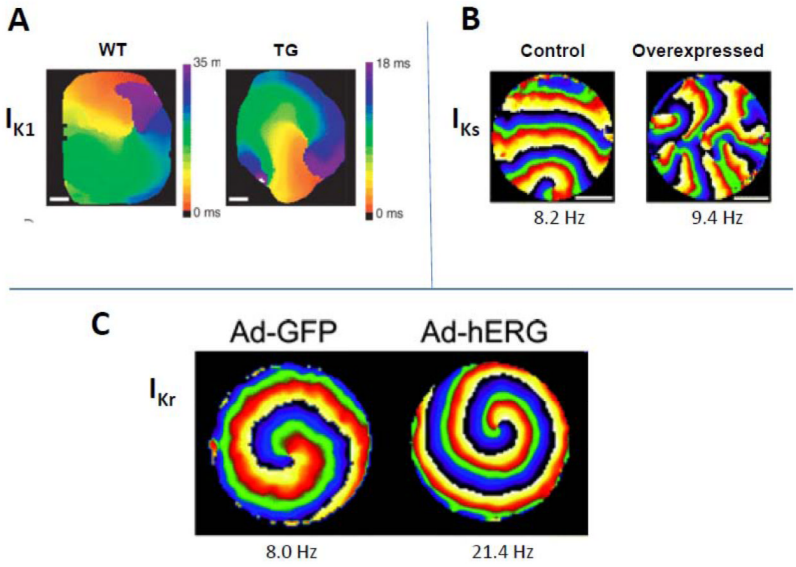

Figure 6.

Rotors, ionic basis. (A.) Rotors in wild-type (WT) and transgenic (TG) mouse hearts where I_{K1} was overexpressed. (From Reference 105) (B.) Rotors in a control NRVM monolayer, and a similar monolayer in which I_{Ks} was overexpressed via adenovirus.[107] (C.) Rotors in a control NRVM monolayer, and a similar monolayer where I_{Kr} was overexpressed via adenovirus. (From reference 108).

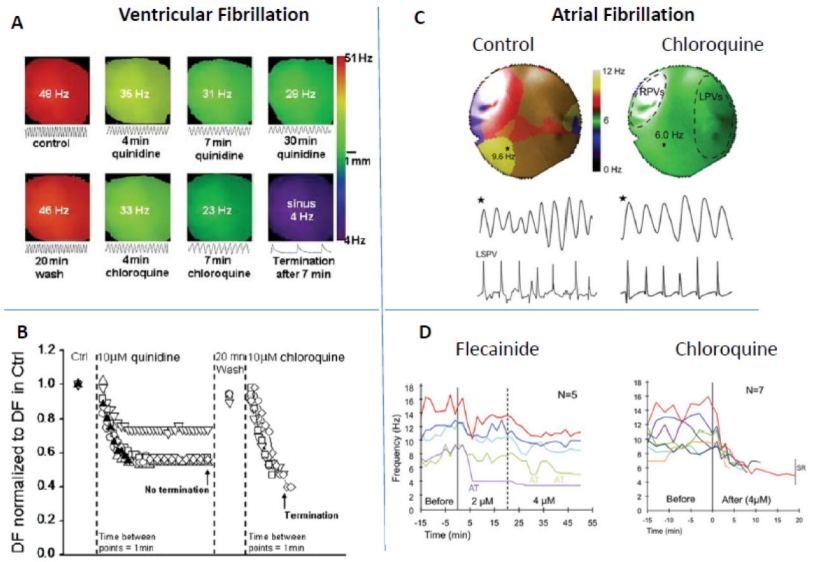

Figure 7.

Rotors and antiarrhythmic drugs in VF and AF. (A.) DF maps of VF in I_{K1} overexpressing TG mice, in the absence and presence of chloroquine. (From Reference 121) (B.) Comparison of quinidine versus chloroquine effects on normalized DF in VF. (From Reference 121) (C.) DF maps and underlying optical/electrical signals during stretch-induced AF in isolated sheep hearts, in control, and in the presence of chloroquine. (From Reference 122) (D.) Comparison of the effects of flecainide and chloroquine on the DF during stretch-induced AF in sheep hearts. (From Reference 122)

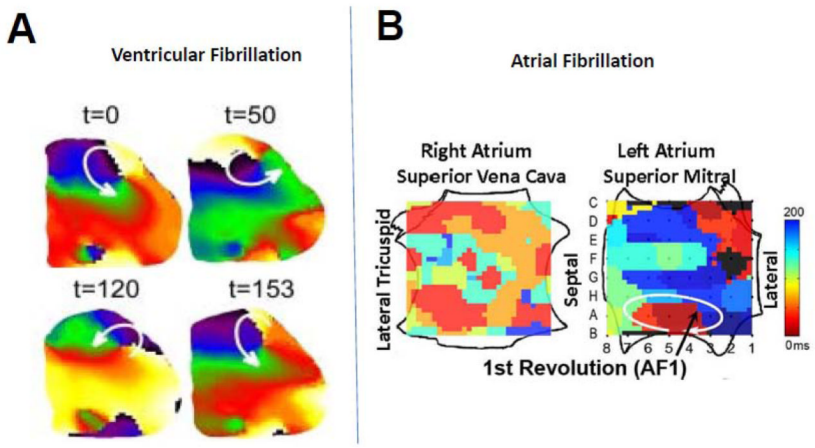

Figure 8.

Rotors in human hearts. (A.) Sequential snapshots during a full rotation of a rotor located near the lateral wall of the left ventricle and generating VF in a human heart mapped optically, in vitro. (From Reference 72). (B.) Left atrial rotor and fibrillatory conduction during AF in a human heart mapped electrically in-vivo using two transvenous basket catheters simultaneously (modified from Reference 129 with permission of the authors and the publisher).